Electronic Supplementary Material (ESI) for Journal of Materials Chemistry C.

Supporting Information

Highly-Efficient Solid-State Emissions of the Anthracene−*o*-Carborane Dyads with Various Substituents and Their Thermochromic Luminescent Properties

Hirofumi Naito[1], Kenta Nishino[1], Yasuhiro Morisaki[1,2], Kazuo Tanaka[1], and Yoshiki Chujo[1]*

[1]*Department of Polymer Chemistry, Graduate School of Engineering, Kyoto University, Katsura, Nishikyo-ku, Kyoto 615-8510, Japan*

[2]*Present address: Department of Applied Chemistry for Environment, School of Science and Technology, Kwansei Gakuin University, 2-1 Gakuen, Sanda, Hyogo 669-1337, Japan*

*E-mail: chujo@chujo.synchem.kyoto-u.ac.jp

Experimental

General. ^{1}H, ^{13}C, and ^{11}B NMR spectra were recorded on a JEOL JNM-EX400 instrument at 400, 100, and 128 MHz, respectively. The ^{1}H and ^{13}C chemical shift values were expressed relative to Me_4Si as an internal standard. The ^{11}B chemical shift values were expressed relative to $BF_3{\cdot}Et_2O$ as an external standard. High-resolution mass spectra (HRMS) were obtained on a Thermo Fisher Scientific EXACTIVE spectrometer for atmospheric pressure chemical ionization (APCI). Analytical thin-layer chromatography (TLC) was performed with silica gel 60 Merck F254 plates. Column chromatography was performed with Wakogel C-300 silica gel. UV−vis absorption spectra were obtained on a SHIMADZU UV3600 spectrophotometer. Photoluminescence (PL) spectra were obtained on a Horiba FluoroMax-4 luminescence spectrometer; absolute PL quantum efficiencies (Φ_{PL}) were determined using a Horiba FL-3018 Integrating Sphere. Fluorescence lifetime measurement was performed on a Horiba FluoreCube spectrofluorometer system; excitation was carried out using a UV diode laser (NanoLED 375 nm). Variable temperature solid-state PL spectra were obtained on an Ocean Optics USB 4000 and recorded on a Cimarec^{TM} Digital Stirring Hotplate. Cyclic voltammetry (CV) was carried out on a BAS CV-50W electrochemical analyzer in DMF containing 0.1 M of sample and 0.1 M of Bu_4NClO_4 with a glassy carbon working electrode, a Pt counter electrode, a Ag/AgCl (Ag/Ag+) reference electrode, and a ferrocene/ferrocenium external reference. X-Ray diffraction (XRD) data were obtained on a Rigaku MiniFlex diffractometer using CuKα radiation in a range of $2 \leq 2\theta \leq 50°$ at intervals of 0.01° at a scanning rate of 0.25° min^{-1}.

Materials. All synthetic procedures were performed under Ar atmosphere. Diethyl ether (Et_2O) and tetrahydrofuran (THF) were purified by passage through purification column under Ar pressure. 1,2-Dimethoxyethane (DME) and diisopropylamine (i-Pr_2NH) were purified by distillation under Ar pressure. *n*-BuLi in hexane, CuCl, pyridine, $Pd(PPh_3)_2Cl_2$, CuI, ethynylbenzene, decaborane ($B_{10}H_{14}$), $AgNO_3$, acetonitrile (MeCN), toluene, iodomethane (MeI), and trimethylsilyl chloride (TMSCl) were obtained commercially and used without purification. 9-(Phenylethynyl)anthracene and 1-(9-anthracenyl)-*o*-carborane (**1**) were synthesized and characterized according to the literature.[1] Poly(methyl methacrylate) (PMMA, M_n = 800,000) was purchased from Nacalai Tesque and used without purification.

Synthetic procedures

1-(9-Anthracenyl)-2-phenyl-*o*-carborane (ANT-Ph). The mixture of 9-(phenylethynyl)anthracene (0.278 g, 1.00 mmol), decaborane (0.257 g, 2.10 mmol), and $AgNO_3$ (6.8 mg, 0.04 mmol) was dissolved in dry toluene (5 mL) at room temperature under Ar atmosphere. MeCN (0.63 mL12.0 mmol) was added, and the mixture was refluxed for 3 d. After cooling to room temperature, the solvent was separated from the solid and evaporated. The residue was subjected to silica gel column chromatography with hexane as an eluent (R_f = 0.21). Recrystallization from $CHCl_3$/MeOH to afford **ANT-Ph** as an orange crystal (0.11 mg, 0.28 mmol, 28%). ^{1}H NMR (400 MHz, CD_2Cl_2): δ (ppm) 9.02 (2H, d, J = 9.0 Hz, Ar-*H*), 8.09 (1H, s, Ar-*H*), 7.74 (2H, d, J = 8.3 Hz, Ar-*H*), 7.52−7.50 (2H, m, Ar-*H*), 7.41−7.32 (2H, m, Ar-*H*), 6.93−6.89 (2H, m, Ar-*H*), 6.58−6.56 (2H, m, Ar-*H*), 4.60−1.56 (10H, br, B-*H*). ^{13}C NMR (100 MHz, CD_2Cl_2): δ (ppm) 134.0, 133.3, 131.8, 130.6, 130.2, 128.6, 127.6, 126.9, 126.1, 125.1, 119.0, 95.7, 91.8. ^{11}B NMR (128 MHz, CD_2Cl_2): δ (ppm) 0.5, –0.7, –2.2, –3.3, –8.5, –9.7, –10.8. HRMS (APCI): Calcd. for $C_{22}H_{24}B_{10}$ $[M+H]^+$ m/z 399.2881, found m/z 399.2879.

1-(9-Anthracenyl)-2-methyl-*o*-carborane (ANT-Me). To a solution of **ANT-H** (64.1 mg, 200 μmol) in 1.60 mL of Et_2O was added dropwise a 1.60 M solution of *n*-BuLi in hexane (125 μL, 200 μmol) at 0 °C under Ar atmosphere. The mixture was stirred for 1 h, and then MeI (40 μL, 640 μmol) was added. The mixture was stirred at room temperature for 4 h in the dark. The reaction mixture was washed with water and brine, and the organic layer was dried over $MgSO_4$. After $MgSO_4$ was removed, the solvent was evaporated. The residue was purified by HPLC with $CHCl_3$ as an eluent and recrystallized from $CHCl_3$/hexane to afford **ANT-Me** as a yellow crystal (25.5 mg, 76.2 μmol, 38%). ^{1}H NMR (400 MHz, CD_2Cl_2): δ(ppm) 9.09 (2H, d, J = 9.3 Hz, Ar-*H*), 8.55 (1H, s, Ar-*H*), 8.00 (2H, t, J = 4.6 Hz, Ar-*H*), 7.56−7.46 (4H, m, Ar-*H*), 4.13−1.08 (10H, br, B-*H*), 0.68 (3H, s, CH_3). ^{13}C NMR (100 MHz, CD_2Cl_2): δ(ppm) 134.1, 133.7, 132.3, 129.0, 127.5, 126.2, 125.4, 119.1, 87.5, 85.6, 22.9. ^{11}B NMR (128 MHz, CD_2Cl_2): δ(ppm) –0.3, –1.5, –4.5, –5.7, –6.6, –8.5, –9.7, –10.8. HRMS (APCI): Calcd. for $C_{17}H_{22}B_{10}$ $[M+H]^+$ m/z 337.2725, found m/z 337.2718.

1-(9-Anthracenyl)-2-trimethylsilyl-*o*-carborane (ANT-TMS). To a solution of **ANT-H** (56.1 mg, 175 μmol) in 1.8 mL of Et_2O was added dropwise a 1.58 M solution of *n*-BuLi in hexane (111 μL, 175 μmol) at 0 °C under Ar atmosphere. The mixture was stirred for 1 h, and then TMSCl (55 μL, 435 μmol) was added, and the mixture was stirred at room temperature for 4 h. The reaction mixture was washed with water and brine, and the organic layer was dried over $MgSO_4$. After $MgSO_4$ was removed, the solvent was evaporated. The residue was purified by HPLC with $CHCl_3$ as an eluent to afford **ANT-TMS** as an orange solid (44.5 mg, 113 μmol, 65%). Single crystals for crystallographic study were obtained by slow evaporation of $CHCl_3$/hexane solution. ^{1}H NMR (400 MHz, CD_2Cl_2): δ(ppm) 9.20 (2H, d, J = 9.3 Hz, Ar-*H*), 8.55 (1H, s, Ar-*H*), 7.96 (2H, dd, J = 8.3, 0.7 Hz, Ar-*H*), 7.58−7.53 (2H, m, Ar-*H*), 7.48 (2H, t, J = 7.4 Hz, Ar-*H*), 4.37−1.29

(10H, br, B-*H*), –0.87 (9H, s, Si-C*H*$_3$). ^{13}C NMR (100 MHz, CD_2Cl_2): δ (ppm) 134.3, 133.8, 132.4, 129.0, 127.1, 126.4, 125.4, 120.6, 88.8, 88.5, –1.4. ^{11}B NMR (128 MHz, CD_2Cl_2): δ (ppm) 1.0, 0.5, –0.1, –6.9, –8.0, –9.1, –10.3. HRMS (APCI): Calcd. for $C_{19}H_{28}B_{10}Si$ $[M+H]^+$ m/z 395.2964, found m/z 395.2958.

Preparation of PMMA dispersion film

PMMA (M_n = 800,000, 30 mg) and the dyads (3 mg) were dissolved in $CHCl_3$ (1 mL), and dispersed film was fabricated via drop casting.

Computational methods

All computations were carried out with the Gaussian 09 suit program.[2] The molecular geometries were investigated by DFT and time-dependent DFT (TD-DFT) calculations with the B3LYP/6-31G(d) level of theory. Calculations on **ANT-H** with the CAM-B3LYP method (more appropriate for donor-acceptor system than the B3LYP method) or using 6-31+G(d) basis set gave similar results described here. The orbital contributions were generated by GaussSum package.[3]

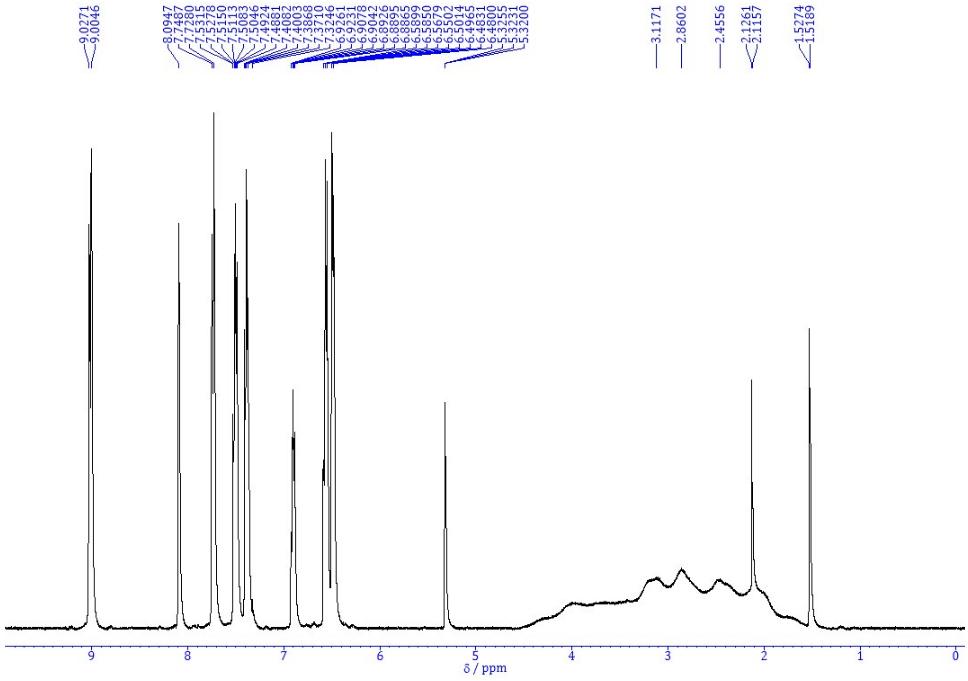

Chart 1. ^{1}H NMR spectrum of **ANT-Ph** in CD_2Cl_2.

Chart 2. ^{13}C NMR spectrum of **ANT-Ph** in CD_2Cl_2.

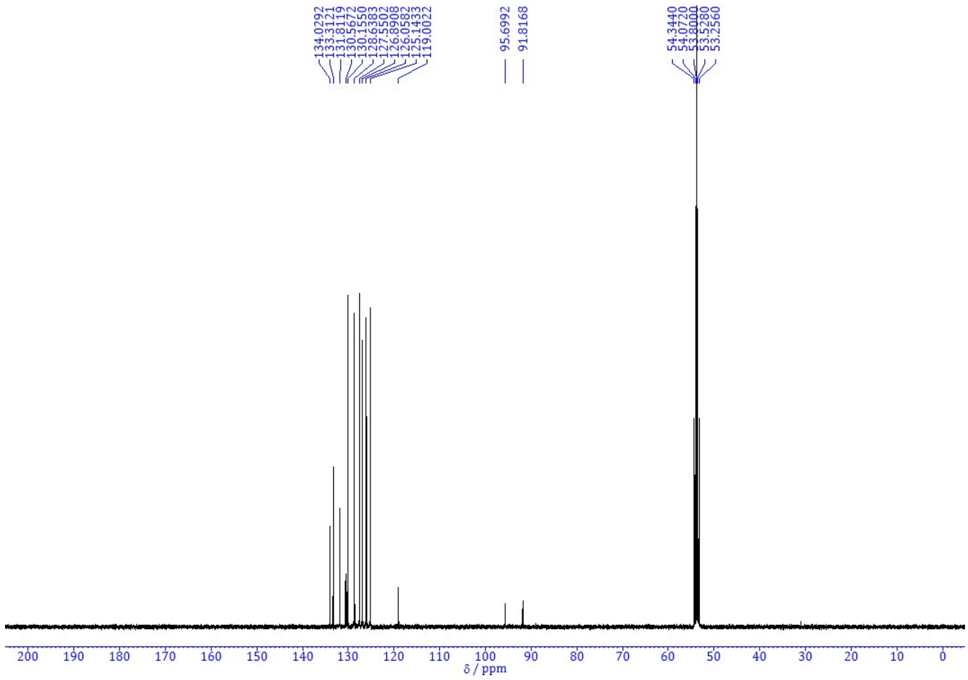

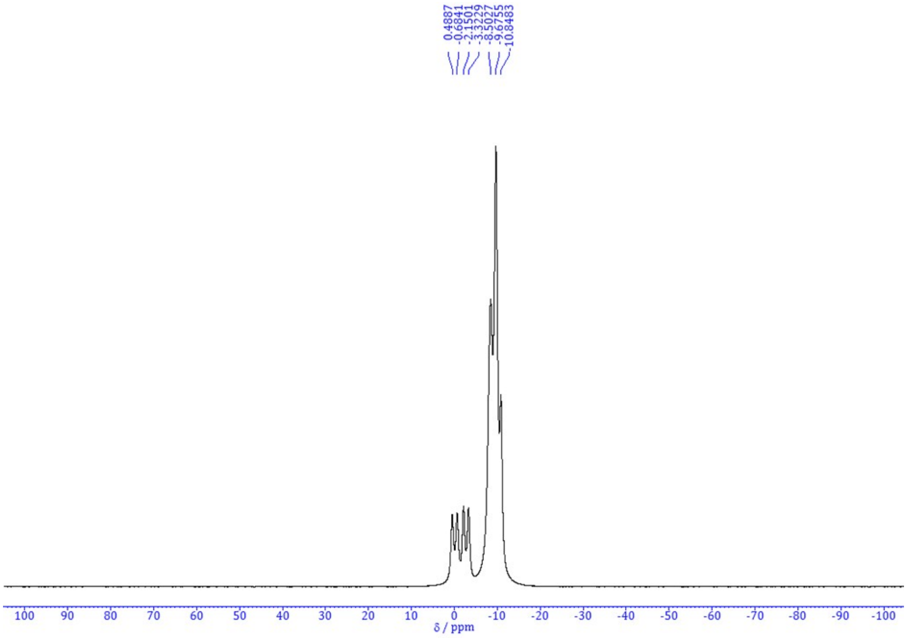

Chart 3. ^{11}B NMR spectrum of **ANT-Ph** in CD_2Cl_2.

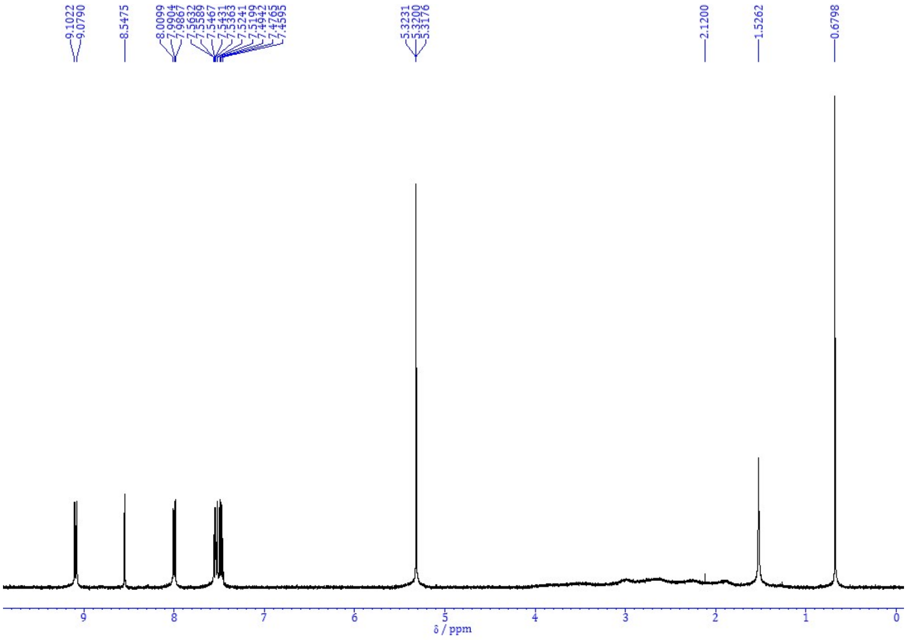

Chart 4. ^{1}H NMR spectrum of **ANT-Me** in CD_2Cl_2.

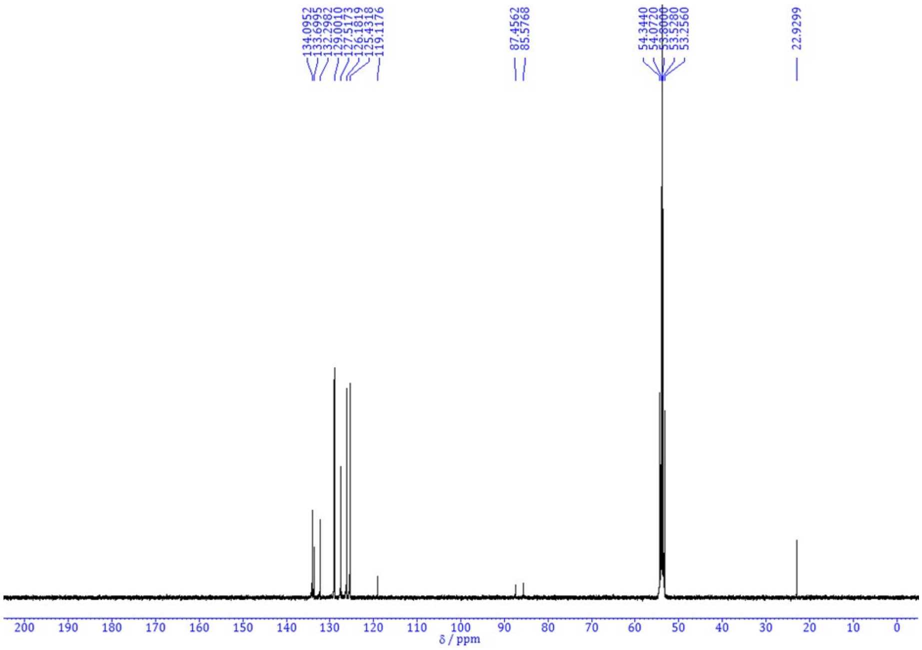

Chart 5. ^{13}C NMR spectrum of **ANT-Me** in CD_2Cl_2.

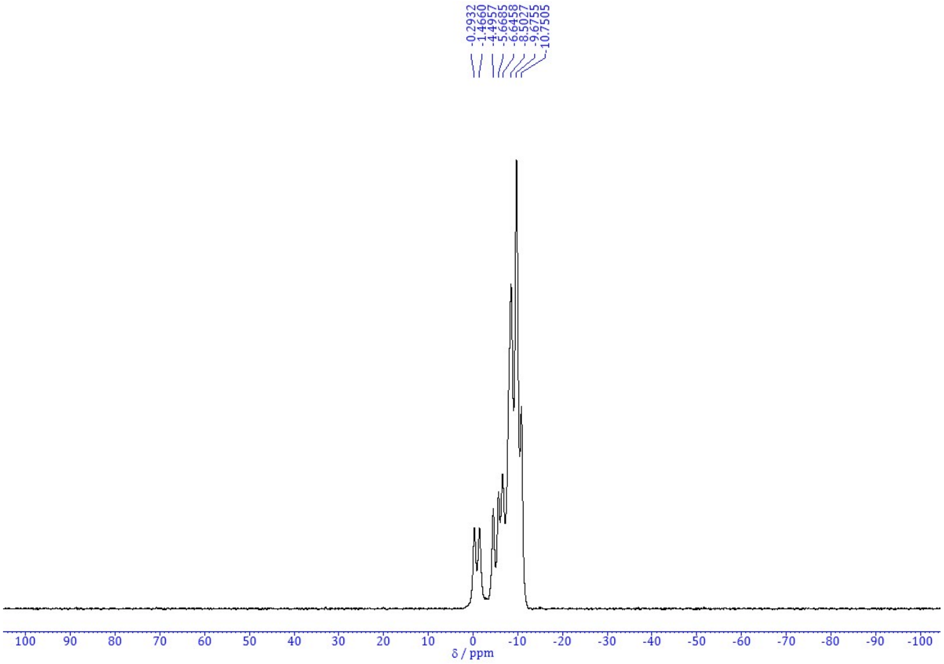

Chart 6. ^{11}B NMR spectrum of **ANT-Me** in CD_2Cl_2.

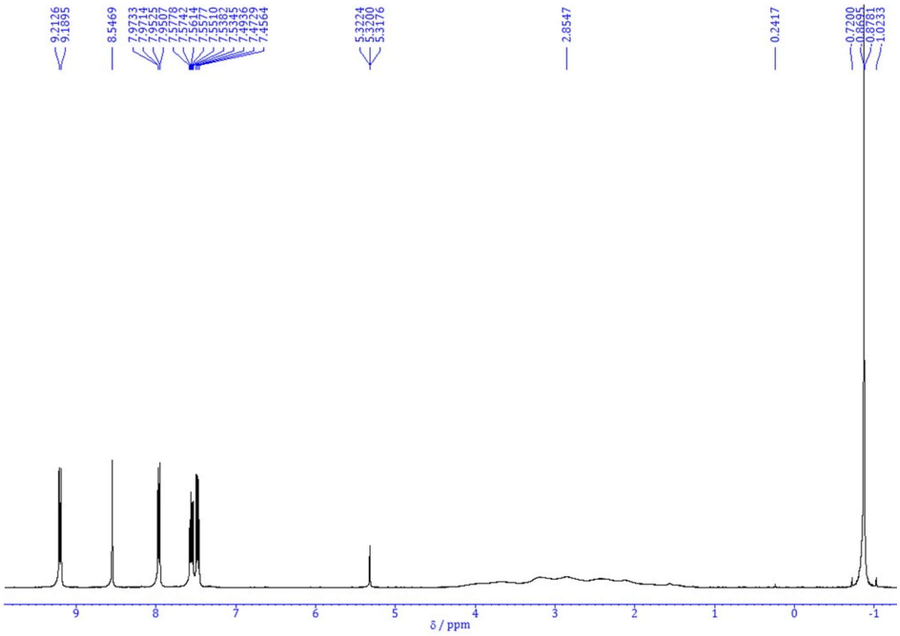

Chart 7. ^{1}H NMR spectrum of **ANT-TMS** in CD_2Cl_2.

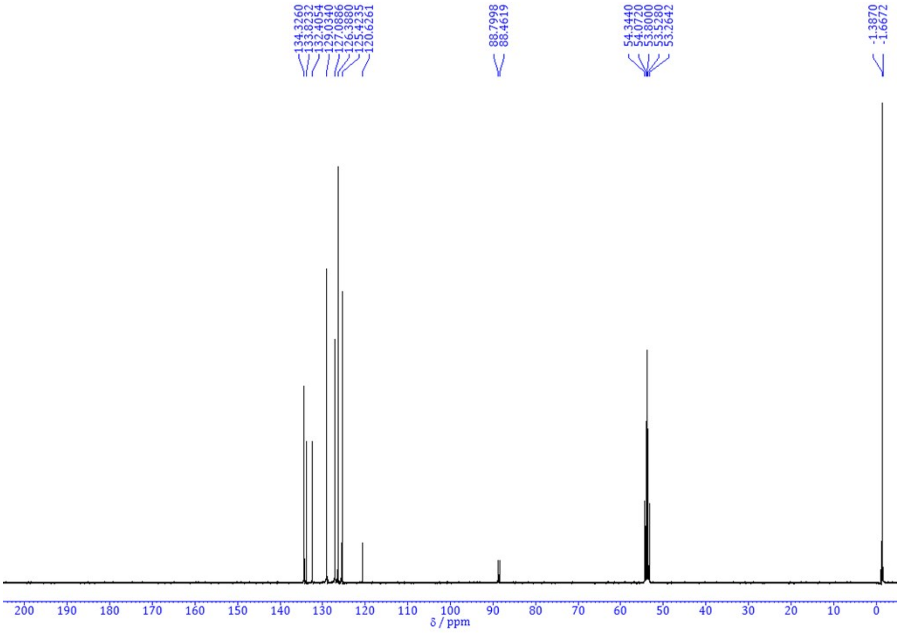

Chart 8. ^{13}C NMR spectrum of **ANT-TMS** in CD_2Cl_2.

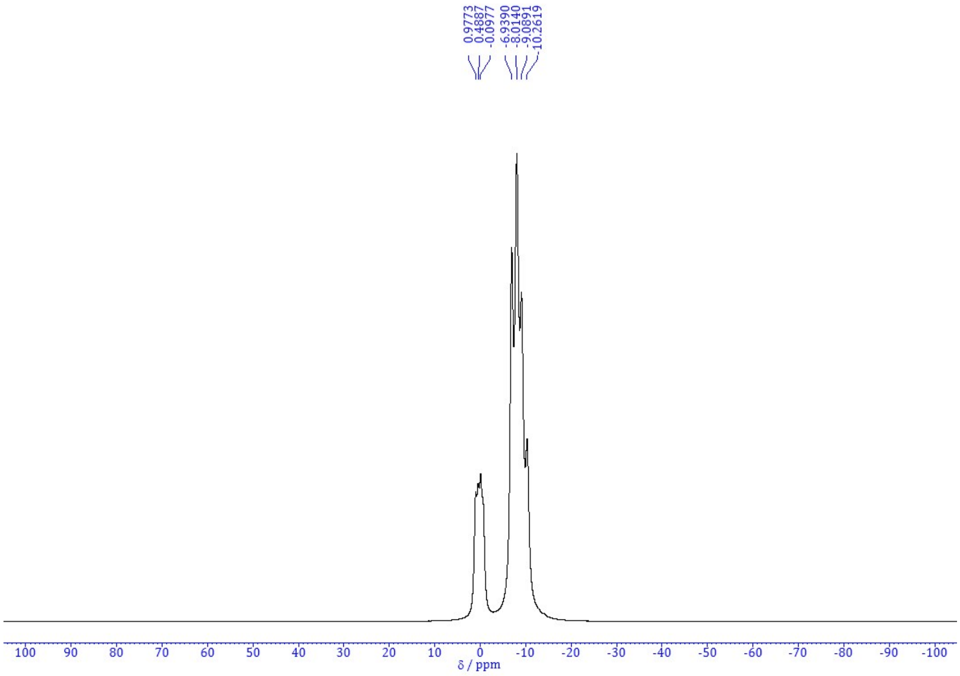

Chart 9. ^{11}B NMR spectrum of **ANT-TMS** in CD_2Cl_2.

Table S1. Crystallographic data of **ANT-Ph**.[a]

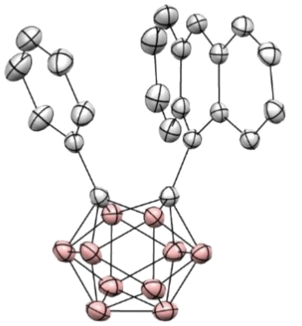

Empirical formula	$C_{22}H_{24}B_{10}$
Formula weight	396.51
Temperature (K)	93(2)
Wavelength (Å)	0.71075
Crystal system, space group	Monoclinic, $P\,2_1/n$
Unit cell dimensions	a = 11.9314(8)
	b = 12.5281(8)
	c = 14.8597(11)
	α = 90
	β = 99.122(7)
	γ = 90
V (Å^3)	2193.1(3)
Z, calculated density (Mg m^{-3})	4, 1.201
Absorption coefficient	0.061
F(000)	824
Crystal size (mm)	0.80 × 0.50 × 0.40
θ range for data collection	3.22-27.48
Limiting indices	$-15\leq h\leq 15$, $-14\leq k\leq 16$, $-19\leq l\leq 19$
Reflections collected (unique)	20669/5026 [R(int) = 0.0766]
Completeness to theta = 27.48	0.999
Max. and min. transmission	0.9760 and 0.9529
Goodness-of-fit on F^2	1.055
Final R indices [$I > 2\sigma(I)$][a]	R_1 = 0.0563, wR_2 = 0.1412
R indices (all data)	R_1 = 0.0790, wR_2 = 0.1552

[a] The structures were solved by direct method (SIR97)[4] and refined by full-matrix least-squares procedures based on F^2 (SHELX-97).[5] [b] $R_1 = \Sigma(|F_0|-|F_c|)/\Sigma|F_0|$. w$R_2 = [\Sigma w(F^2{}_0-F^2{}_c)^2/\ \Sigma w(F^2{}_0)^2]^{1/2}$. $w = 1/[\sigma^2(F^2{}_0)+[(ap)^2+bp]]$, where $p = [\max(F^2{}_0,0)+2F^2{}_c]/3$.

Table S2. Crystallographic data of **ANT-Me**.[a]

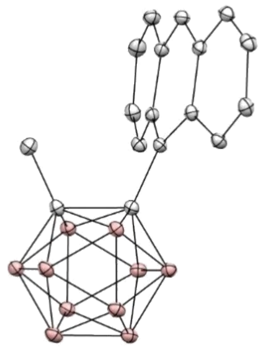

Empirical formula	$C_{17}H_{22}B_{10}$
Formula weight	334.45
Temperature (K)	93(2)
Wavelength (Å)	0.71075
Crystal system, space group	Orthorhombic, $P\,2_1\,2_1\,2_1$
Unit cell dimensions	$a = 7.4049(3)$
	$b = 10.2673(4)$
	$c = 23.6399(11)$
	$\alpha = 90$
	$\beta = 90$
	$\gamma = 90$
V (Å^3)	1797.30(13)
Z, calculated density (Mg m^{-3})	4, 1.236
Absorption coefficient	0.061
F(000)	696
Crystal size (mm)	0.60 × 0.50 × 0.50
θ range for data collection	3.25-27.42
Limiting indices	$-9 \leq h \leq 9$, $-12 \leq k \leq 13$, $-30 \leq l \leq 30$
Reflections collected (unique)	17403/4099 [R(int) = 0.0386]
Completeness to theta = 27.48	0.997
Max. and min. transmission	0.9700 and 0.9642
Goodness-of-fit on F^2	1.036
Final R indices [$I > 2\sigma(I)$][a]	$R_1 = 0.0376$, w$R_2 = 0.0956$
R indices (all data)	$R_1 = 0.0399$, w$R_2 = 0.0970$

[a] The structures were solved by direct method (SIR97)[4] and refined by full-matrix least-squares procedures based on F^2 (SHELX-97).[5] [b] $R_1 = \Sigma(|F_0|-|F_c|)/\Sigma|F_0|$. w$R_2 = [\Sigma w(F^2_0-F^2_c)^2/\ \Sigma w(F^2_0)^2]^{1/2}$. $w = 1/[\sigma^2(F^2_0)+[(ap)^2+bp]]$, where $p = [\max(F^2_0,0)+2F^2_c]/3$.

Table S3. Crystallographic data of **ANT-TMS**.[a]

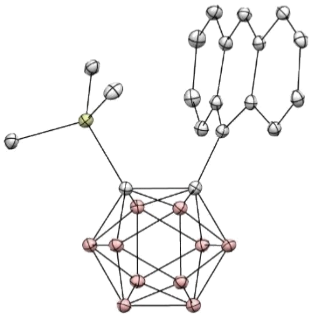

Empirical formula	$C_{19}H_{28}B_{10}Si$
Formula weight	392.60
Temperature (K)	93(2)
Wavelength (Å)	0.71075
Crystal system, space group	Monoclinic, $P\ 2_1/a$
Unit cell dimensions	$a = 10.1119(5)$
	$b = 16.5353(8)$
	$c = 12.9542(7)$
	$\alpha = 90$
	$\beta = 90.332(6)$
	$\gamma = 90$
V (Å^3)	2165.95(19)
Z, calculated density (Mg m^{-3})	4, 1.204
Absorption coefficient	0.113
F(000)	824
Crystal size (mm)	0.90 × 0.80 × 0.50
θ range for data collection	3.15-27.48
Limiting indices	$-13 \leq h \leq 13$, $-20 \leq k \leq 21$, $-16 \leq l \leq 16$
Reflections collected (unique)	18646/4926 [R(int) = 0.0592]
Completeness to theta = 27.47	0.996
Max. and min. transmission	0.9456 and 0.9051
Goodness-of-fit on F^2	0.997
Final R indices [$I > 2\sigma(I)$]^a	$R_1 = 0.0456$, w$R_2 = 0.1147$
R indices (all data)	$R_1 = 0.0580$, w$R_2 = 0.1255$

[a] The structures were solved by direct method (SIR97)[4] and refined by full-matrix least-squares procedures based on F^2 (SHELX-97).[5] [b] $R_1 = \Sigma(|F_0|-|F_c|)/\Sigma|F_0|$. w$R_2 = [\Sigma w(F^2{}_0-F^2{}_c)^2/\ \Sigma w(F^2{}_0)^2]^{1/2}$. $w = 1/[\sigma^2(F^2{}_0)+[(ap)^2+bp]]$, where $p = [\max(F^2{}_0,0)+2F^2{}_c]/3$.

Table S4. Optical and electrochemical properties of the dyads

Compound	UV/vis[a]			CV[d]		
	λ_{abs} (nm) (ε, $\times 10^{-4}$ M^{-1} cm^{-1})[b]	$\lambda_{abs,edge}$ (nm)	E_g (eV)[c]	E_{onset}^{red} (V)[e]	HOMO (eV)[f]	LUMO (eV)[g]
ANT-H	267(10.7), 395(0.86)	433	2.86	–1.21	–6.45	–3.59
ANT-Ph	271(6.8), 408(0.66)	463	2.68	–1.00	–6.48	–3.80
ANT-Me	268(12.5), 403(0.95)	448	2.77	–1.21	–6.36	–3.59
ANT-TMS	268(8.9), 404(0.73)	449	2.76	–1.10	–6.46	–3.70

[a] Measured in THF solution (1.0×10^{-5} M) at room temperature. [b] Molar extinction coefficient. [c] Band gap energy: $E_g = 1240 / \lambda_{abs,\ edge}$. [d] CV was carried out in DMF with 0.1 M Bu_4NClO_4 as supporting electrolyte. [e] Onset potential of first reduction wave. [f] HOMO = LUMO – E_g (eV). [g] Calculated from the empirical formula, LUMO = $-E^{red} - 4.80$ (eV).[6]

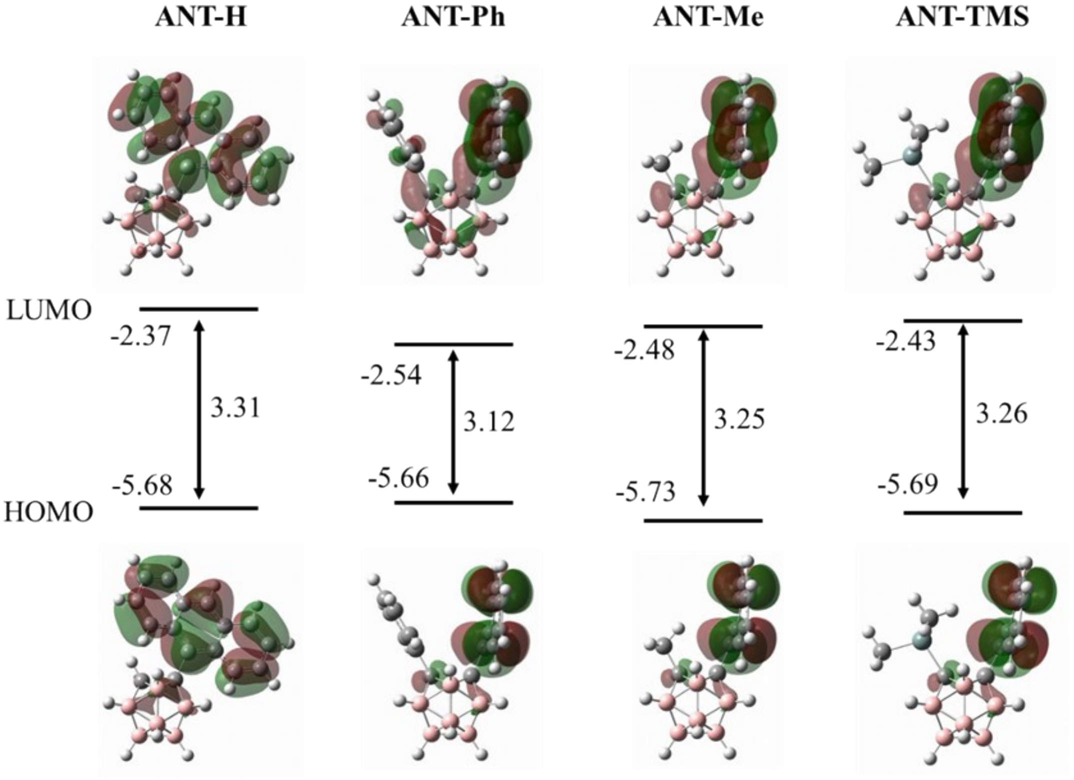

Figure S1. Frontier orbitals and their energies (eV) of the dyads.

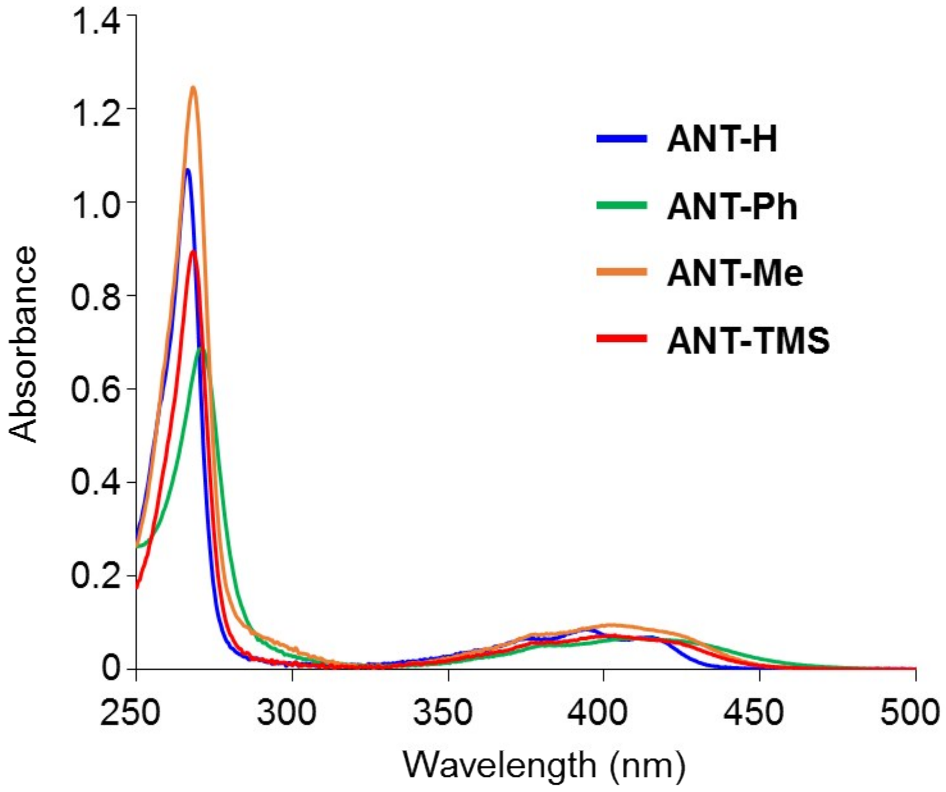

Figure S2. UV−vis absorption spectra of the dyads in THF (1.0×10^{-5} M).

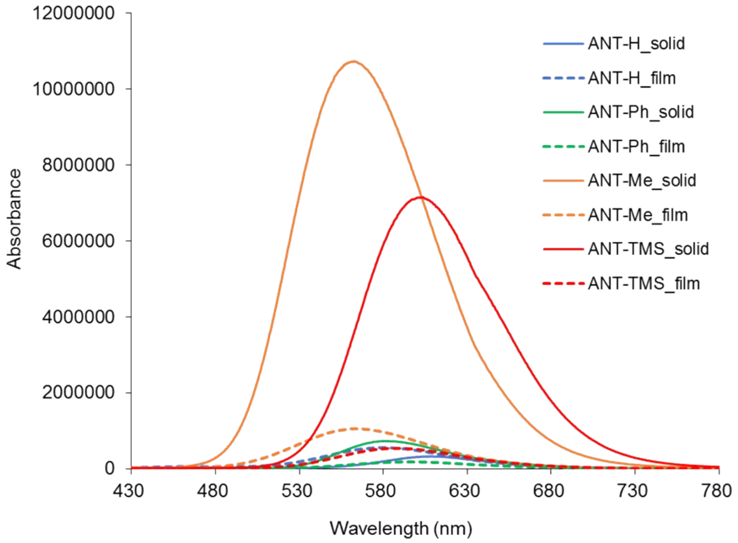

Figure S3. PL spectra of the dyads in the crystalline state and PMMA (10 wt%).

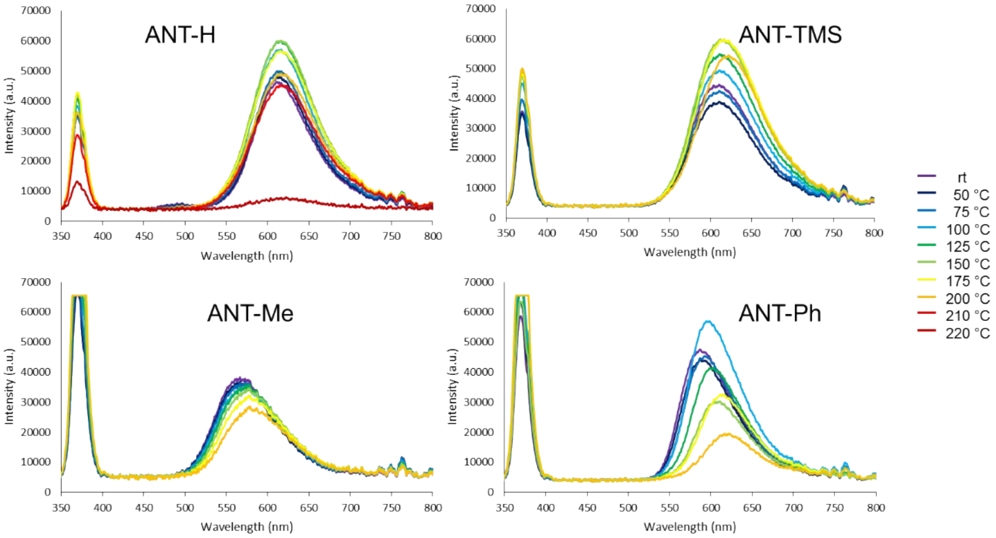

Figure S4. Emission spectra of the powder samples of the *o*-carborane dyads during heating.

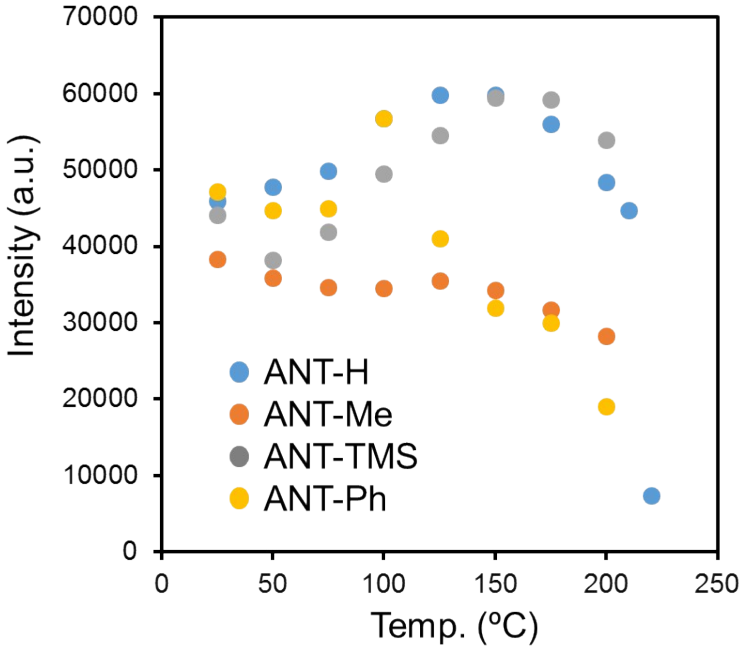

Figure S5. Changes in emission intensity of the dyads by heating at the peak top in the emission spectra.

Table S5. Thermal decomposition temperatures of the dyads[a]

dyads	T_{d5} (°C)
ANT-H	200
ANT-Me	201
ANT-TMS	223
ANT-Ph	268

[a] Determined from the decomposition temperature with 5 wt% weight losses with the thermogravimetric analyses under nitrogen flow (200 mL/min).

References

1. Finke, A. D.; Elleby, E. C.; Boyd, M. J.; Weissman, H.; Moore, J. S. *J. Org. Chem.* **2009**, *74*, 8897-8900.

2. Gaussian 09, Revision **D.01**, M. J. Frisch, G. W. Trucks, H. B. Schlegel, G. E. Scuseria, M. A. Robb, J. R. Cheeseman, G. Scalmani, V. Barone, B. Mennucci, G. A. Petersson, H. Nakatsuji, M. Caricato, X. Li, H. P. Hratchian, A. F. Izmaylov, J. Bloino, G. Zheng, J. L. Sonnenberg, M. Hada, M. Ehara, K. Toyota, R. Fukuda, J. Hasegawa, M. Ishida, T. Nakajima, Y. Honda, O. Kitao, H. Nakai, T. Vreven, J. A. Montgomery, Jr., J. E. Peralta, F. Ogliaro, M. Bearpark, J. J. Heyd, E. Brothers, K. N. Kudin, V. N. Staroverov, R. Kobayashi, J. Normand, K. Raghavachari, A. Rendell, J. C. Burant, S. S. Iyengar, J. Tomasi, M. Cossi, N. Rega, J. M. Millam, M. Klene, J. E. Knox, J. B. Cross, V. Bakken, C. Adamo, J. Jaramillo, R. Gomperts, R. E. Stratmann, O. Yazyev, A. J. Austin, R. Cammi, C. Pomelli, J. W. Ochterski, R. L. Martin, K. Morokuma, V. G. Zakrzewski, G. A. Voth, P. Salvador, J. J. Dannenberg, S. Dapprich, A. D. Daniels, Ö. Farkas, J. B. Foresman, J. V. Ortiz, J. Cioslowski, and D. J. Fox, Gaussian, Inc., Wallingford CT, 2009.

3. O'boyle, N. M.; Tenderholt, A. L.; Langner, K. M. *J. Comput. Chem.* **2008**, *29*, 839-845.

4. A. Altomare, M. C. Burla, M. Camalli, G. Cascarano, C. Giacovazzo, A. Guagliardi, A. G. Moliteni, G. Polidori, R. Spagna, *J. Appl. Cryst.* **1999**, *32*, 115-119.

5. Sheldrick, G. M. *SHELX-97 Programs for Crystal Structure Analysis* (University of Göttingen, Göttingen, Germany, 1997).

6. Chen, C.-P.; Chan, S.-H.; Chao, T.-C.; Ting, C.; Ko, B.-T. *J. Am. Chem. Soc.* **2008**, *130*, 12828-12833.